Low-complexity Detectors for Cyclic Structured Space-time Block Coded Spatial Modulation over a Slow Rayleigh Fading Channel

Dickson O. Egbune[1], Babatunde S. Adejumobi[1,2], Isaac O. A. Omeiza[1,3], Frank A. Ibikunle[1], Adeniyi Olayanju[1], Ayodele S. Oluwole[4], and Thokozani Shongwe[2]
[1] Department of Electrical and Information Engineering, Landmark University, Omu-Aran, Nigeria
[2]Centre for Telecommunication, Department of Electrical and Electronic Engineering Science, University of Johannesburg, Johannesburg 2092, South Africa
[3]Department of Electrical and Electronic Engineering, University of Ilorin, Kwara State, Nigeria.
[4]Department of Electrical and Electronic Engineering, Federal University, Oye-Ekiti, Nigeria
Email: {egbune.dickson, omeiza.isaac, ibikunle.francis}@lmu.edu.ng; {adejumobibabatunde, soluwole}@gmail.com; tshongwe@uj.ac.za

Abstract —This paper presents low-complexity detectors for space-time block coded spatial modulation with cyclic structured (STBC-CSM) codeword over a quasi-static frequency-flat Rayleigh fading channel. Two low-complexity detectors are proposed, which reduce the computational complexity of the STBC-CSM maximum-likelihood (ML) detector and demonstrate near-ML error performance of STBC-CSM. Furthermore, Monte-Carlo simulation results for the proposed schemes are presented to validate the theoretical Average Bit Error Probability (ABEP) of STBC-CSM. The proposed low-complexity detectors can achieve a 99% reduction in computational complexity, when high order M-ary ($M > 64$) amplitude and/or phase modulation symbols are employed for STBC-CSM.

Index Terms—Low-complexity detector, maximum-likelihood, Rayleigh fading channel, space-time block codes, space-time block coded spatial modulation

I. Introduction

Modern-day multimedia services demand increased data rate, improved error performance and better quality of service for real-time applications, which are constituents of the 5G system. To satisfy these demands, researchers have concentrated efforts to ensure that there are advancements and improvements in Multiple-Input Multiple-Output (MIMO) and massive-MIMO systems. Several MIMO techniques in the form of index modulation systems have been presented in the literature, which offers improved error performance and throughput to MIMO systems. For example, in [1], [2], Space Shift Keying (SSK) modulation, which exploits antenna indexes to improve the error performance of MIMO have been presented, while a generalized form of SSK has been presented in [3]. More recently, index modulation systems like Space-Time Block Coded (STBC) spatial modulation (STBC-SM) [4] has been proposed. STBC-SM combines the advantages of Alamouti STBC and SM [5] techniques to improve the error performance of both schemes, while the spectral efficiency of Alamouti STBC is improved. In a similar manner as STBC, STBC-SM transmits two symbols x_p and x_q , employing two timeslots.

Several schemes based on the STBC-SM technique have been proposed in the literature. For example, a high rate STBC-SM for 4 and 6 transmit antenna has been presented in [6], while STBC-SM and media-based STBC-SM, which employ labeling diversity was proposed in [7] and [8], respectively, to improve the error performance of STBC-SM. Of uttermost interest is STBC-SM with cyclic structured codeword (STBC-CSM) [9]. STBC-CSM employs codeword rotation to increase the spectral efficiency of STBC-SM. However, this increase in spectral efficiency comes at a cost, as the computational complexity of the system is increased significantly, when the ML detector is employed. The joint ML detector searches all possible amplitude and/or phase modulation (APM) symbol pairs and across all possible transmit antenna pairs, to estimate the transmit antenna pair and the transmitted symbol pair.

Based on this background, this paper proposes low-complexity detectors, which reduce the computational complexity of the optimal ML detector for STBS-CSM detection significantly and offer near-ML error performance of STBC-CSM over a slow, frequency-flat Rayleigh fading channel.

The detectors employ the orthogonality of STBC-CSM codeword as an advantage, to reduce the computational complexity of STBC-CSM detection. Furthermore, a near-ML detector, which is independent of the constellation size of the APM employed is proposed, thus demonstrating a significantly reduced computational complexity, when compared to other detectors. Finally, the Monte Carlo simulation results to validate the

Manuscript received December 20, 2019; revised September 23, 2020.
Corresponding author email: adejumobi.babatunde@lmu.edu.ng
doi:10.12720/jcm.15.11.818-825

theoretical average bit error probability (ABEP) of STBC-CSM are presented. The rest of this paper have the following organization: Section II gives a background of the STBC-CSM system, while the theoretical analysis of STBC-CSM is presented in Section III. The proposed low complexity detectors for STBC-CSM are presented in Section IV, while the computational complexity analysis in terms of complex operations is performed for STBC-CSM in Section V. The numerical results of the proposed low-complexity detectors to validate the theoretical ABEP of STBC-CSM are discussed in Section VI. Finally, Section VII concludes the paper.

Notations: We have employed the following notations in this paper; matrices and vectors are represented by bold uppercase letters and bold lowercase letters, respectively. The notations $(\cdot)^*$ $(\cdot)^T$, $(\cdot)^H$, $\mathcal{R}(.)$ and $\|\cdot\|_F$ represent conjugate, transpose, Hermittian, the real part of a complex number and Frobenius norm, respectively. The quantization slicing function is denoted as $\mathcal{D}(\cdot)$, while $\boldsymbol{I}_w$ is a $w \times w$ identity matrix, having all elements in its diagonal as unity.

II. Background of STBC-CSM

Like STBC-SM, STBC-CSM employs a pair of transmit antennas from a group of N_T transmit antennas to transmit a pair of amplitude and/or phase modulation (APM) symbols. In STBC-CSM, the symbols x_{q_1} and x_{q_2} , $p_i, q_i \in [1{:}M]$ are taken from two constellation sets $\boldsymbol{\Omega}_1$ and a rotated version of $\boldsymbol{\Omega}_1$ which is given as, $\boldsymbol{\Omega}_2 = \boldsymbol{\Omega}_1 e^{j\theta}$respectively, where$i \in [1{:}2]$ and M is the constellation size of the M-ary APM employed. The spectral efficiency of STBC-CSM is given as [9]:

$$\delta_{csm/sm} = 0.5\log_2 c + \log_2 M \tag{1}$$

where $c = \lfloor N_T (N_T - 1) \rfloor 2_P$ for STBC-CSM, whereas $\left\lfloor c = \frac{\lfloor N_T\ (N_T - 1)\rfloor}{2} \right\rfloor 2p$ for STBC-SM, c represents the total number of usable codewords for STBC-CSM and STBC-SM. N_T is the total number of transmit antennas employed by STBC-CSM and STBC-SM. Hence, the spectral efficiency offered by the spatial domain of STBC-CSM and STBC-SM is $0.5\log_2 c$.

In STBC-CSM, the transmit antenna pair tx_1 and tx_2, for $tx_1, tx_2 \in [1{:}N_T]$ are employed to transmit two symbols x_{p_1} and x_{p_2}, respectively, during Timeslot 1. In Timeslot 2, the conjugates of the transmitted symbols for Timeslot 1, $x_{q_2} = -\left(x_{q_1} e^{j\theta_k}\right)^*$ and $x_{p_2} = \left(x_{p_1} e^{j\theta_k}\right)^*$are transmitted by the same transmit antenna pair tx_1 and tx_2, respectively.

The total number of STBC-CSM codewords comprise of $a, a \in [1{:}N_T - 1]$ codebooks, each codebook consist of b, $b \in [1{:}N_T]$ codewords. The b-th codeword of the a-th codebook of STBC-CSM may be formulated as [9]:

$$\boldsymbol{\chi}_{a,b} = G^{b-a} D a^{e^{j\theta a}} \tag{2}$$

where $\boldsymbol{G}$ is an $N_T \times N_T$ right-shift circular matrix, such that $\boldsymbol{G}^0 = \boldsymbol{I}_{N_T}$, θ_a is the rotational angle for the a-th codebook, while $\boldsymbol{D}_a$ is an $N_T \times 2$ matrix, which may be defined as [9]:

$$\boldsymbol{D}_a = \begin{array}{c} \begin{bmatrix} x_{p_1} & 0 & \cdots & x_{q_1} & \cdots & 0 \\ x_{q_2} & 0 & \cdots & x_{p_2} & \cdots & 0 \end{bmatrix} \\ \downarrow \\ \text{the } (1+k)-th \text{ column} \end{array} \tag{3}$$

Given the τ - th, $\tau \epsilon [1{:}c]$ $N_T \times 2$ STBC-CSM codeword $\boldsymbol{\chi}_\tau$, the received signal vector of STBC-CSM for the i- th, $i\epsilon[1{:}2]$ timeslot may be represented as [9]:

$$\overline{\boldsymbol{y}}_i = \sqrt{\frac{\rho}{2}} \boldsymbol{H}_i \boldsymbol{\chi}_i^\tau + \boldsymbol{\eta}_i \tag{4}$$

where $\sqrt{\frac{\rho}{2}}$ denotes the average signal-to-noise ratio (SNR) at the receiver, $\overline{\boldsymbol{y}}_1$ represents the $N_R \times 1$ received signal vector for the i-th timeslot, $\boldsymbol{\chi}_i^\tau$ is the $N_T \times 1$ transmit vector for Timeslot i. η_i denotes an $N_R \times 1$ independent and identically distributed AWGN vector at the receiver during the i-th timeslot. $\boldsymbol{H}_i$ is the $N_R \times N_T$ channel matrix for Timeslot i. The expression for the received signal in (4) can be further simplified as [10]:

$$\overline{\boldsymbol{y}}_1 = \sqrt{\frac{\rho}{2}} \left(\boldsymbol{h}_{\tau,tx_1}^1 x_{p1} + \boldsymbol{h}_{\tau,tx_2}^1 x_{q_1} \right) + \boldsymbol{\eta}_1 \tag{5a}$$

$$\overline{\boldsymbol{y}}_2 = \sqrt{\frac{\rho}{2}} \left(\boldsymbol{h}_{\tau,tx_2}^2 (x_{p_1})^* - \boldsymbol{h}_{\tau,tx_1}^2 (x_{q_1})^* \right) + \boldsymbol{\eta}_2 \tag{5b}$$

where $\boldsymbol{h}_{\tau,tx_1}^i$ and $\boldsymbol{h}_{\tau,tx_2}^i$, for $i \in [1{:}2]$ are tx_1-th and tx_2-th $N_T \times 1$ column vectors of the channel matrix $\boldsymbol{H}_i$ during Timeslot i. The optimal ML detector for STBC-CSM may be represented as:

$$[\hat{\tau}, \hat{p}, \hat{q}] = \underset{\substack{\hat{\tau} \in [1:c], \\ \hat{x}_p \in \Omega_1, \hat{x}_q \in \boldsymbol{\Omega}_2}}{\operatorname{argmin}} \left(\left\| \overline{\boldsymbol{y}}_1 - \sqrt{\frac{\rho}{2}} \left(\boldsymbol{h}_{\tau,tx_1}^1 x_{p_1} + \boldsymbol{h}_{\tau,tx_2}^1 x_{q_1} \right) \right\|_F^2 + \left\| \overline{\boldsymbol{y}}_2 - \sqrt{\frac{\rho}{2}} \left(\boldsymbol{h}_{\tau,tx_2}^2 x_{p_1}^* - \boldsymbol{h}_{\tau,tx_1}^2 x_{q_1}^* \right) \right\|_F^2 \right) \tag{6}$$

where $\hat{\tau}$, $\hat{p}$ and $\hat{q}$ are estimates of τ, p and q, respectively. The expression in (6) is reduced to become [10]:

$$\begin{aligned} [\hat{\tau}, \hat{p}, \hat{q}] = {} & \sqrt{\frac{\rho}{2}} \left\| \boldsymbol{g}_{p_1} \right\|_F^2 + \sqrt{\frac{\rho}{2}} \left\| \boldsymbol{g}_{q_1} \right\|_F^2 - 2\mathcal{R}\left(\overline{\boldsymbol{y}}_1^H \boldsymbol{g}_{p_1}\right) - 2\mathcal{R}\left(\overline{\boldsymbol{y}}_1^H g_{q_1}\right) + \sqrt{2p\boldsymbol{\mathcal{R}}}\left(\left(g_{p_1}\right)^H g_{p_1} \right) + \sqrt{\frac{\rho}{2}} \left\| \boldsymbol{g}_{q_2} \right\|_F^2 \\ & + \sqrt{\frac{\rho}{2}} \left\| \boldsymbol{g}_{p_2} \right\|_F^2 - 2\boldsymbol{\mathcal{R}}\left(\overline{\boldsymbol{y}}_1^H g_{q_2}\right) - 2\boldsymbol{\mathcal{R}}\left(\overline{\boldsymbol{y}}_1^H \boldsymbol{g}_{p_2}\right) + \sqrt{2p\boldsymbol{\mathcal{R}}}\left(\left(\boldsymbol{g}_{q_2}\right)^H \boldsymbol{g}_{p_2} \right) \end{aligned} \tag{7}$$

where $\boldsymbol{g}_{p_1} = \boldsymbol{h}^1_{\tau,tx_1} x_{p_1}$ $\boldsymbol{g}_{q_1} = \boldsymbol{h}^1_{\tau,tx_2} x_{q_1}$ $\boldsymbol{g}_{q_2} = -\boldsymbol{h}^2_{\tau,tx_1} x^*_{q_1}$, $\boldsymbol{g}_{p_2} = \boldsymbol{h}^2_{\tau,tx_2} x^*_{p_1}$.

III. Analysis of Theoretical ABEP for STBC-CSM

For the purpose of comparison, the theoretical ABEP of an $N_T \times N_R$ STBC-CSM system over a fast frequency-flat Rayleigh fading (FFRF) channel is given as [10]:

$$\text{ABEP} \leq \frac{1}{cM^2} \sum_{\boldsymbol{U}} \sum_{\widehat{\boldsymbol{U}}} \frac{N_{\boldsymbol{U}\widehat{\boldsymbol{U}}}\, P\big(\boldsymbol{U} \longrightarrow \widehat{\boldsymbol{U}}\big)}{\log_2 c + 2\log_2 M} \tag{8}$$

where $P\big(\boldsymbol{U} \longrightarrow \widehat{\boldsymbol{U}}\big)$ is the pairwise error probability (PEP) event, such that the transmitted codeword $\boldsymbol{U}$ is received erroneously as $\widehat{\boldsymbol{U}}$. $N_{\boldsymbol{U}\widehat{\boldsymbol{U}}}$ is the number of bits in error which corresponds to the PEP event $P\big(\boldsymbol{U} \longrightarrow \widehat{\boldsymbol{U}}\big)$. $\boldsymbol{U}$ is the $N_T \times 2$ transmit codeword having x_{p_i}, $i \in [1{:}\,2]$ and x_{q_i} as the only non-zero elements in the i-th column corresponding to the tx_1-th and tx_2-th positions, respectively. $\widehat{\boldsymbol{U}}$ is an erroneous received version of $\boldsymbol{U}$. The PEP $P\big(\boldsymbol{U} \longrightarrow \widehat{\boldsymbol{U}}\big)$ of STBC-CSM is given as [10]:

$$\begin{aligned} P\big(\boldsymbol{U} \longrightarrow \widehat{\boldsymbol{U}}\big) = \frac{1}{2n}\Bigg[\frac{1}{2}\left(\prod_{\boldsymbol{i=1}}^{2} M\left(\frac{1}{2}\right)\right) \\ + \sum_{v=1}^{\boldsymbol{n-1}}\left(\prod_{i=1}^{\boldsymbol{2}} M_{\boldsymbol{i}}\left(\frac{1}{2sin^2\theta_v}\right)\right)\Bigg] \end{aligned} \tag{9}$$

where $M_i(\psi) = \left(\frac{1}{1+2\psi\,\sigma^2_{\alpha_i}}\right)^{N_R}$, $i \in [1{:}\,2]$ $\sigma^2_{\alpha_i} = \frac{\rho}{8}\|x_i\|^2_F$, and $\theta_v = \frac{v\pi}{2g}$. n represents an arbitrarily large number of iteration that is needed for the convergence of the trapezoidal approximation of the Q-function. $\boldsymbol{x}_i$ is the difference between the i–th column of $\boldsymbol{U}$ and $\widehat{\boldsymbol{U}}$.

IV. Low-Complexity Detectors for STBC-CSM

In this section, low-complexity detectors for STBC-CSM are presented, while two near-ML error performance detectors are proposed to reduce the computational complexity of the optimal ML detector over a slow, frequency-flat Rayleigh fading channel

A. *Low-complexity ML detector (Detector 1)*

Considering a $N_R \times N_T$ M-QAM STBC-CSM system where $N_T = 3$ and the number of codeword, $c = 4$. Assume that the selected codeword is $\boldsymbol{\chi}_\tau$, $\tau \in [1{:}\,c]$, the received signal vector for the first and second timeslots $\bar{\boldsymbol{y}}_1$ and $\bar{\boldsymbol{y}}_2$, respectively, can be viewed as a $2N_R \times 1$ receive signal vector y which may be formulated as [8]:

$$\mathbf{y} = \begin{bmatrix} \bar{\boldsymbol{y}}_1 \\ \bar{\boldsymbol{y}}_2 \end{bmatrix} = \sqrt{\frac{\rho}{2}}\boldsymbol{\mathcal{H}}_\tau \begin{bmatrix} x_{p_1} \\ x_{q_1} \end{bmatrix} + \widehat{\boldsymbol{n}} \tag{10}$$

where $\bar{\boldsymbol{y}}_1 = \begin{bmatrix} \bar{\boldsymbol{y}}^1_1 & \bar{\boldsymbol{y}}^1_2 & \cdots & \bar{y}^1_{N_R} \end{bmatrix}^T$ and $\bar{\boldsymbol{y}}_2 = \begin{bmatrix} \bar{y}^2_1 & \bar{y}^2_2 & \cdots & \bar{y}^2_{N_R} \end{bmatrix}^T$ are $N_R \times 1$ signal vectors for Timeslots 1 and 2, respectively. $\boldsymbol{\mathcal{H}}_\tau$ is a $2N_R \times 2$ channel matrix modified in a similar method as [3]. $\boldsymbol{h}_{tx_1}$ and $\boldsymbol{h}_{tx_2}$ are the channel vectors for the τ-th, $\tau \in [1 : c]$ transmit antenna pair tx_1 and tx_2, respectively. It is derived from the column vectors $\boldsymbol{h}_{tx_1}$ and $\boldsymbol{h}_{tx_2}$, for $tx_1, tx_2 \in [1{:}\,N_T]$ of the channel matrix $\boldsymbol{H} = [\boldsymbol{h}_1 \quad \boldsymbol{h}_2 \quad \cdots \quad \boldsymbol{h}_{N_T}]$. The elements of the channel matrix $\boldsymbol{H}$**,** are i.i.d with zero mean and unit variance $CN(0,1)$.

Given that $N_T = 3$, the different modified channel realizations $\boldsymbol{\mathcal{H}}_\tau$ for STBC-CSM may be formulated as [3], 7]:

$$\boldsymbol{\mathcal{H}}_1 = \begin{bmatrix} h_{1,1} & h_{1,2}\Phi \\ h^*_{1,2} & -h^*_{1,1}\Phi \\ h_{2,1} & h_{2,2}\,\Phi \\ h^*_{2,2} & -h^*_{2,1}\Phi \\ \vdots & \vdots \\ h_{N_R,1} & h_{N_R,2}\Phi \\ h^*_{N_R,2} & -h^*_{N_R,1}\Phi \end{bmatrix}$$

$$\boldsymbol{\mathcal{H}}_2 = \begin{bmatrix} h_{1,2} & h_{1,3}\Phi \\ h^*_{1,3} & -h^*_{1,2}\Phi \\ h_{2,2} & h_{2,3}\,\Phi \\ h^*_{2,3} & -h^*_{2,2}\Phi \\ \vdots & \vdots \\ h_{N_R,2} & h_{N_R,3}\Phi \\ h^*_{N_R,3} & -h^*_{N_R,2}\Phi \end{bmatrix}$$

$$\boldsymbol{\mathcal{H}}_3 = \begin{bmatrix} h_{1,1}\varphi_2 & h_{1,3}\mathcal{Z}_2 \\ h^*_{1,3}\varphi^*_2 & -h^*_{1,1}\mathcal{Z}^*_2 \\ h_{2,1}\varphi_2 & h_{2,3}\,\mathcal{Z}_2 \\ h^*_{2,3}\varphi^*_2 & -h^*_{2,1}\mathcal{Z}^*_1 \\ \vdots & \vdots \\ h_{N_R,1\varphi_2} & h_{N_R,3}\mathcal{Z}_2 \\ h^*_{N_R,3}\varphi^*_2 & -h^*_{N_R,1}\mathcal{Z}^*_2 \end{bmatrix}$$

$$\boldsymbol{\mathcal{H}}_4 = \begin{bmatrix} h_{1,2\varphi_2} & h_{1,1}\mathcal{Z}_2 \\ h^*_{1,1\varphi^*_2} & -h^*_{1,2}\,\mathcal{Z}^*_2 \\ h_{2,2\varphi_2} & h_{2,1}\mathcal{Z}_2 \\ h^*_{2,1}\varphi^*_2 & -h^*_{2,2}\mathcal{Z}^*_2 \\ \vdots & \vdots \\ h_{N_R,2\varphi_2} & h_{N_R,1}\,z_2 \\ h^*_{N_R,1\varphi^*_2} & -h^*_{N_R,2}\,\mathcal{Z}^*_2 \end{bmatrix} \tag{11}$$

where $h_{m,n}$, for $m \in [1{:}\,N_R]$, and $n \in [1{:}\,N_T]$ is the channel fading coefficient for the link between m–th receive antenna and the n-th transmit antenna, $\Phi = e^{j\theta}$ is the rotation angle of the APM constellation $\boldsymbol{\Omega}_2$. $\mathcal{Z}_k = \varphi_k\,\Phi$ and $\mathcal{Z}^*_k = \varphi^*_k\Phi$ given that $\varphi_k = e^{j\theta_k}$, $k\epsilon[1{:}\,N_T - 1]$ is the rotation angle corresponding to the k– th codebook where the τ–th codeword is located. Hence, the low-complexity optimal ML detector may be represented as [4], [11]:

$$[x^1_\tau \quad w^1_\tau] = \underset{x_{p_1} \in \boldsymbol{\Omega}_1}{\text{argmin}} \left\|\boldsymbol{g}_{x_1}\right\|^2_F - 2\mathcal{R}\big(\boldsymbol{y}^H\,\boldsymbol{g}_{x_1}\big) \tag{12a}$$

$$[x_\tau^2 \quad w_\tau^2] = \underset{x_{q_1} \in \mathbf{\Omega}_1}{\operatorname{argmin}} \left\|\boldsymbol{g}_{x_2}\right\|_F^2 - 2\mathcal{R}\left(\boldsymbol{y}^H \boldsymbol{g}_{x_2}\right) \quad (12b)$$

where $\boldsymbol{g}_{x_1} = \sqrt{\frac{\rho}{2}} \mathfrak{H}_\tau^1 x_{p_1}$ and $\boldsymbol{g}_{x_2} = \sqrt{\frac{\rho}{2}} \mathfrak{H}_\tau^2 x_{q_1}$, $\mathfrak{H}_\tau^i$ is a $2N_R \times 1$ channel vector obtained from the i-th column of the modified channel matrix $\boldsymbol{\mathcal{H}}_\tau$, such that $\boldsymbol{\mathcal{H}}_\tau = [\mathfrak{H}_\tau^1 \quad \mathfrak{H}_\tau^2]$, w_τ^1 and w_τ^2 are the associated minimum ML metrics of the estimates x_τ^1 and x_τ^2, $\boldsymbol{y}$ is the $2N_R \times 1$ modified received signal vector given in (10). The joint detection ofτ, x_1 and x_2 is performed by calculating the minimum ML metric, which is given as [4]:

$$\left[\hat{\tau}, \hat{x}_{p_1}, \hat{x}_{q_1}\right] = \underset{\tau \in [1:x]}{\operatorname{argmin}} (w_\tau^1 + w_\tau^2) \quad (13)$$

where $\hat{\tau}$, $\hat{x}_{p_1}$ and $\hat{x}_{q_1}$ are estimates of τ, x_{p_1} and x_{q_1}, respectively.

B. Proposed Simple Low-complexity Near-ML Detector for STBC-CSM)Detector 2)

To detect the symbols, the orthogonality of the codeword is employed as an advantage [4]. Firstly, the metric $\tilde{z}_\tau$ is computed and is defined as [12]:

$$\tilde{\boldsymbol{z}}_\tau = \begin{bmatrix} \tilde{z}_\tau^1 \\ \tilde{z}_\tau^2 \end{bmatrix} = \boldsymbol{\mathcal{H}}_\tau^H \boldsymbol{y} \quad (14)$$

Then, the estimates v_τ^1 and v_τ^2 are obtained from the equalized symbols defined as [12]:

$$v_\tau^1 = \frac{\tilde{z}_\tau^1}{\|\mathfrak{H}_\tau^1\|_F^2} \quad (15a)$$

$$v_\tau^2 = \frac{\tilde{z}_\tau^2}{\|\mathfrak{H}_\tau^2\|_F^2} \quad (15b)$$

where $\mathfrak{H}_\tau^i$, $i \in [1:2]$ corresponds to the i-th column of the matrix $\boldsymbol{\mathcal{H}}_\tau$. The estimates of the transmitted symbols x_τ^1 and x_τ^2 corresponding to the τ- th transmit antenna pair of tx_1 and tx_2 is obtained by employing the quantization slicing function $\mathcal{D}(\cdot)$ on v_τ^1 and v_τ^2 given as [10]:

$$[p_\tau \quad x_\tau^1] = \mathcal{D}(v_\tau^1) \quad (16a)$$

$$[q_\tau \quad x_\tau^2] = \mathcal{D}(v_\tau^2) \quad (16b)$$

where p_τ and q_τ for $p_\tau, q_\tau \in [1:M]$, are the corresponding indexes of the symbols x_τ^1 and x_τ^2, respectively. x_τ^1 x_τ^2 are the most likely candidate pair of the transmitted symbols x_{p_1} and x_{q_1}, respectively, for the τ–th transmit antenna pair. To conclude Stage 1 of the proposed detection, this process is performed for the c possible antenna pairs. Stage 2 of the detection involves a joint ML detection. It is achieved by performing an exhaustive search across the c possible antenna pairs, employing the corresponding symbol estimates x_τ^1 and x_τ^2 obtained in Stage 1. The Joint ML detector optimizes the metric, which is defined as [12]:

$$[\hat{\tau}, \quad \hat{x}_{p_1}, \quad \hat{x}_{q_1}] = \underset{\tau \in [1:c]}{\operatorname{argmin}} \left(\left\| \boldsymbol{y} - \sqrt{\frac{\rho}{2}} \boldsymbol{\mathcal{H}}_\tau \begin{bmatrix} x_\tau^1 \\ x_\tau^2 \end{bmatrix} \right\|_F^2 \right) \quad (17)$$

C. Proposed QR Decomposition (QRD) Near-ML Detector for STBC-CSM

Similar to [13], the modified channel matrix $\boldsymbol{\mathcal{H}}_\tau$ may be expressed as [14]:

$$\sqrt{\frac{\rho}{2}} \boldsymbol{\mathcal{H}}_\tau = \boldsymbol{Q}_\tau \boldsymbol{R}_\tau \quad (18)$$

where $\boldsymbol{Q}_\tau$ is a $2N_R \times 2N_R$ matrix and $\boldsymbol{R}_\tau$ is a $2N_R \times 2$ upper triangular matrix, both of which are obtained from the QRD of $\boldsymbol{\mathcal{H}}_\tau$. In order to achieve low-complexity detection, firstly, the most likely candidate pair x_τ^1 and x_τ^2 of the transmitted symbols x_{p_1} and x_{q_1}, respectively, for the τ–th transmit antenna pair are estimated by [14]:

$$x_1^\tau = \underset{x_{p_1} \in \mathbf{\Omega_1}}{\operatorname{argmin}} \left\|(\boldsymbol{Q}_\tau)^H \boldsymbol{y} - \boldsymbol{R}_{\tau_1} x_{p_1}\right\|_F^2 \quad (19a)$$

$$x_2^\tau = \underset{x_{q_1} \in \mathbf{\Omega}_1}{\operatorname{argmin}} \left\|(\boldsymbol{Q}_\tau)^H \boldsymbol{y} - \boldsymbol{R}_{\tau_2} x_{q_1}\right\|_F^2 \quad (19b)$$

where $\boldsymbol{R}_{\tau_i}$ is the i–th column of $\boldsymbol{R}_\tau$. Then, a joint ML detection across all likely candidate symbol pair is performed and is given by:

$$[\hat{\tau}, \quad \hat{x}_{p,} \quad \hat{x}_q] = \underset{\substack{\tau \in [1:c] \\ x_1^\tau \in \mathbf{\Omega}_1, x_2^\tau \in \mathbf{\Omega}_1}}{\operatorname{argmin}} \left(\left\| \boldsymbol{Q}_\tau^H \boldsymbol{y} - \boldsymbol{R}_\tau \begin{bmatrix} x_1^\tau \\ x_2^\tau \end{bmatrix} \right\|_F^2 \right) \quad (20)$$

V. Computational Complexity Analysis

In this section, the computational complexity of the different low-complexity schemes in terms of complex multiplication [15], is performed and analyzed.

A. Computational Complexity of STBC-CSM Detector 1

Considering the optimal ML detector given in (7), each term performs N_R multiplications. Since there are 10 terms, it makes the computational complexity to be $10N_R$ multiplications for a single iteration. The two Frobenius norm operators having $N_R \times 1$ vector involves an additional $2N_R$ complex multiplications and $2N_R - 2$ complex additions. These operations described, must be performed over cM^2 iterations, since the ML detector needs to perform an exhaustive search over all possible symbol and transmit antenna pairs, thus making it a total of [10]:

$$\delta_{ML} = cM^2(12N_R - 2) \quad (21)$$

B. Computational Complexity of STBC-CSM Detector 1

Detector 1, which is the optimal ML low-complexity detector employs a minimum $4N_R$ complex multiplications and $2N_R - 1$ complex additions to obtain $\|\boldsymbol{g}_{x_i}\|_F^2$, $i \in [1{:}2]$. Furthermore, to determine the metric $\boldsymbol{y}^H \boldsymbol{g}_{x_i}$, $2N_R$ complex multiplication and $2N_R - 1$ complex addition is performed. The operations in (13) is ignored, since it does not involve complex operations. As can be seen from (12), these operations are performed for c possible codewords and for M possible symbol pairs, hence, the total computational complexity for this detector may be given as:

$$\delta_{optimal} = 4cM^2(5N_R - 1) \quad (22)$$

C. Computational Complexity of STBC-CSM Detector 2

Employing the proposed method of subsection B, the metric $\tilde{z}_\tau$ in (14) is determined by $4N_R$ complex multiplication and $2N_R$ complex addition. Furthermore, υ_τ^1 and υ_τ^2 is determined by performing a total of $4N_R$ complex multiplication and $4N_R - 2$ complex addition. Since the operations in (16) requires a one-to-one mapping, it is excluded from the computational complexity. Hence the total computational complexity of Stage 1 may be represented as:

$$\delta_{stage1} = 2c(7N_R - 1) \quad (23)$$

The operations performed in Stage 2 is similar to detection in (7), however, this process is performed over c iterations. Hence, the computational complexity for Stage 2 is given as:

$$\delta_{stage2} = 2c(6N_R - 1) \quad (24)$$

Hence, the computational complexity for this scheme is given as:

$$\delta_{near-ML} = \delta_{stage1} + \delta_{stage2} = 2c(13N_R - 2) \quad (25)$$

D. Computational Complexity of QRD STBC-CSM Detector

The QRD detector for STBC-CSM is given in (18) - (20). The QR factorization algorithm employed is presented in line 3-16, page 34 of [16]. Furthermore, since we know that our modified channel matrix $\boldsymbol{\mathcal{H}}_\tau$ matrix is a $2N_R \times 2$ matrix, the QR factorization employs $2N_R$ norms, which results in $2N_R$ complex multiplications for calculating the diagonal entries of the $\boldsymbol{R}$ matrix. The computation employed in achieving items (12) and (13) of the referenced QR algorithm employs $4N_R^2(2N_R - 1)$ complex multiplication and another $4N_R^2(2N_R - 1)$ complex addition. Since the QR factorization has to be performed for c iterations, the computational complexity needed to perform the QR factorization may be represented as:

$$\delta_{QR_{fac}} = 16N_R^3 - 4N_R^2 \quad (26)$$

To perform the operation in (19), it requires $4N_R^2 + 4N_R + 3M$ complex multiplication and another $4N_R^2 - 2N_R + 3M$ complex addition. It is noteworthy that the operations of Stage1 of the QRD detector δ_{stage1} given in (18) and (19) must be carried out for c iterations. Hence, the computational complexity of Stage 1 may be represented as:

$$\delta_{stage1} = c(16N_R^3 + 4N_R^2 + 2N_R + 6M) \quad (27)$$

To determine the received symbol pair from the c most likely estimate pairs, as presented in (20), we must bear in mind that the value for $\boldsymbol{Q}_\tau^H \boldsymbol{y}$ and $\boldsymbol{R}_\tau$ are stored. Hence, there is no need to recalculate it. However, there is need to perform $2N_R + 3$ complex multiplication and another 3 complex addition. Since this search is performed over c iterations, then, the computational complexity for Stage 2 of the QRD detector δ_{stage2} may be presented as:

$$\delta_{stage2} = c(2N_R + 6) \quad (28)$$

Hence, the total computational complexity for the QRD δ_{QR} may be represented as:

$$\begin{aligned}\delta_{QRD} &= \delta_{stage1} + \delta_{stage2} \\ &= 2c(8N_R^3 + 2N_R^2 + 2N_R \\ &\quad + 3M + 3)\end{aligned} \quad (29)$$

Hence, the total computational complexity for the QRD δ_{QR} may be represented as:

TABLE I. COMPUTATIONAL COMPLEXITY REDUCTION WITH RESPECT TO THE OPTIMAL ML DETECTOR

Parameters	Optimal ML	Detector 1	Reduction	Detector 2	Reduction	QRD	Reduction
$N_R = 2, M = 4$	1,408	576	59.1%	200	85.8%	728	48.3%
$N_R = 2, M = 8$	5,632	1,152	79.5%	200	96.4%	824	85.4%
$N_R = 2, M = 16$	22,528	2,304	89.8%	200	99.1%	1,006	95.5%
$N_R = 4, M = 4$	2,944	1,216	58.7%	408	86.1%	4,536	-54.1%
$N_R = 4, M = 8$	11,776	2,432	79.3%	408	96.5%	4,632	60.7%
$N_R = 4, M = 16$	47,104	4,864	89.7%	408	99.1%	4,824	89.8%

$$\delta_{QRD} = \delta_{stage1} + \delta_{stage2} = 2c(8N_R^3 + 2N_R^2 + 2N_R + 3M + 3) \quad (30)$$

A summary of the computational complexities, for the different detectors of STBC-CSM over a slow, frequency-flat Rayleigh fading channel is given in Table I. Furthermore, the computational complexities of the different low-complexity schemes, in terms of the total number of complex operations performed are presented. Also, in Table I, the percentage reduction in computational complexity with respect to the optimal ML detector has been presented.

A constant value of $c = 4$, has been employed to calculate the computational complexities of the low-complexity schemes given in Table I, while varying the values of N_R and M. This is because the scalar "c" is a constant multiplier among all the detectors.

Considering the proposed detectors, the computational complexity of the detectors improves significantly with increase in the APM modulation order. The most effective low-complexity detector of the detectors presented is the proposed Detector 2, having 85.8% reduction in the computational complexity, even with few receive antennas. This is because the Detector 2 is independent of the APM modulation order. For example, when $N_R = 2$ and $M = 4, 8$ and 16, the computational complexity involved 200 complex operations. A change in the computational complexity was observed only after the number of receive antennas was changed.

As can be seen from Table I, the QRD detector is more effective than the optimal ML detector at higher modulation order, when a reduced number of receive antennas is employed. For example, when $N_R = 2$ and $M = 4$, the QRD detector achieves a 48% reduction, while the computational complexity of the QRD detector increase beyond the optimal ML detector by 54.1%.

VI. Numerical Result

In this section, the simulation results for the different low-complexity schemes are presented employing Monte Carlo simulation. The BER performances of the proposed low-complexity detectors are compared with the average BER of the optimal ML detector and the theoretical results for the union bound BER performance.

For the simulation, the following assumptions have been made; full knowledge of the channel is available at the receiver, the channels are an independent and identically distributed slow, frequency-flat Rayleigh fading channel. The receiver encounters AWGN, while the transmitted symbols are taken from a gray coded M-QAM constellation. Furthermore, the transmit and receive antennas are separated wide enough to avoid correlation between the antennas of the transceiver system.

In Fig. 1 and Fig. 2, the BER performance of 16-QAM STBC-CSM, employing 5×4 and 3×4 transceiver antenna configuration system are presented, respectively.

Concerning Fig. 1, where $N_T = 5$, and the number of usable codewords is 16. As expected, the plots demonstrate a tight match between the different near-ML low-complexity schemes and the optimal ML scheme (ML). For example, when the BER of STBC-CSM is 10^{-3}, there are no vivid difference between the optimal ML scheme and the different near ML low-complexity detectors. As the BER improves further to 10^{-5}, the difference between the proposed near-ML detectors and the optimal ML detector are also unnoticeable. The evaluated theoretical union bound (Theory) for fast FFRF channel also demonstrate close results.

In Fig. 2, the number of transmit antennas $N_T = 3$ and the number of usable codewords are 4.

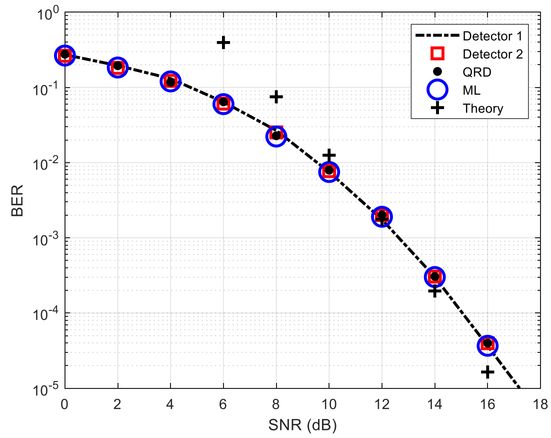

Fig. 1 BER performances of STBC-CSM for N_T = 5, c = 16, N_R = 4 and M = 16

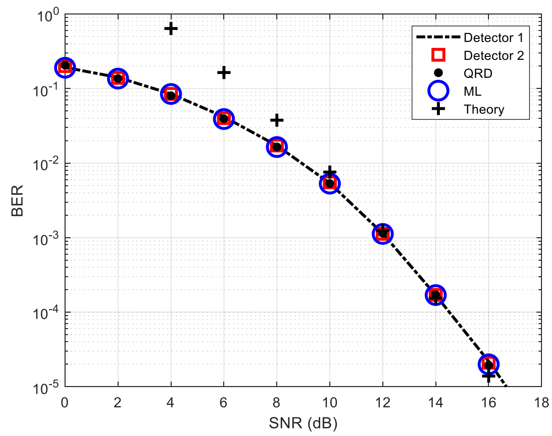

Fig. 2. BER performances of STBC-CSM for N_T = 3, c = 4, N_R = 4 and M = 16

Similar to Fig. 1, the BER of the optimal ML detector in Fig. 2 demonstrate a close match with the low complexity detectors, having no noticeable difference in the different plots.

VII. Conclusions

This paper has presented three near-ML low-complexity detection schemes for STBC–CSM. The numerical results presented have demonstrated a tight match between the error performance of the proposed detectors and that of the optimal ML detector, even at low SNR. In addition, the computational complexity of the different detectors discussed were formulated. The low-complexity near-ML detectors offered significantly reduced computational complexity of approximately 99% than the optimal ML detector. Hence, requiring significantly lower processing power for the receiver.

Conflict of Interest

The authors declare no conflict of interest.

Author Contributions

DO conducted the research; DO, BS original draft; BS, IO supervision; FA, A, AS, T review and editing; all authors had approved the final version.

References

[1] J. Jeganathan, "SPACE shift keying modulation for MIMO channels," PhD thesis, Concordia University, 2008.

[2] B. S. Adejumobi and N. Pillay, "Quadrature spatial modulation orthogonal frequency division multiplexing," *Journal of Telecommunication, Electronic and Computer Engineering*, vol. 10, no. 4, pp. 51-57, 2018.

[3] J. Jeganathan, A. Ghrayeb, and L. Szczecinski, "Generalized space shift keying modulation for MIMO channels," in *Proc., IEEE 19th International Symposium on Personal, Indoor and Mobile Radio Communications*, 2008, pp. 1–5.

[4] E. Basar, U. Aygolu, E. Panayirci, and H. V. Poor, "Space-time block coded spatial modulation," *IEEE Transactions on Communications*, vol. 59, no. 3, pp. 823–832, 2011.

[5] R. Y. Mesleh, H. Haas, S. Sinanovic, C. W. Ahn, and S. Yun, "Spatial modulation," *IEEE Transactions on Vehicular Technology*, vol. 57, no. 4, pp. 2228–2241, 2008.

[6] M. T. Le, V. D. Ngo, H. A. Mai, and X. N. Tran, "High-rate space-time block coded spatial modulation," in *Proc., International Conference on Advanced Technologies for Communications*, Vietnam, 2012, pp. 278–282.

[7] K. Govindasamy, H. Xu, and N. Pillay, "Space-time block coded spatial modulation with labeling diversity," *International Journal of Communication Systems*, 2018.

[8] B. S. Adejumobi and T. Shongwe, "Labeling diversity for media-based space-time block coded spatial modulation," *IEEE Access*, vol. 8, pp. 99870-99879, 2020

[9] X. Li and L. Wang, "High rate space-time block coded spatial modulation with cyclic structure," *IEEE Communications Letters*, vol. 18, no. 4, pp. 532–535, 2014.

[10] B. S. Adejumobi and N. Pillay, "Low-Complexity detection for space-time block coded spatial modulation with cyclic structure," *Journal of Communications*, vol. 13, pp. 391–395, 2018.

[11] B. S. Adejumobi, N. Pillay, and S. H. Mneney, "A study of spatial media-based modulation using RF mirrors," in *Proc. IEEE AFRICON*, Cape Town, South Africa, 2017, pp. 336–341.

[12] H. Xu and N. Pillay, "Simple near-maximum-likelihood low-complexity detection scheme for Alamouti space-time block coded spatial modulation," *IET Communications*, vol. 8, no. 15, pp. 2611–2618, 2014.

[13] J. Yoon, D. Shin, and J. Park, "A low-complexity composite QR decomposition architecture for MIMO detector," in *Proc. IEEE International Symposium on Circuits and Systems*, Australia, 2014, pp. 1692–1695.

[14] A. Chauhan and R. Mehra, "Analysis of QR Decomposition for MIMO Systems," in *Proc. International Conference on Electronic Systems, Signal Processing and Computing Technologies*, India, 2014, pp. 69–73.

[15] B. S. Adejumobi and N. Pillay, "RF mirror media-based space-time block coded spatial modulation techniques for two time-slots," *IET Communications*, vol. 13, no. 15, pp. 2313–2321, 2019.

[16] A. M. Elshokry, "Complexity and performance evaluation of detection schemes for spatial multiplexing MIMO systems," PhD thesis, The Islamic University, 2010.

Dickson Ogochukwu Egbune received his B.Eng. in Electrical /Electronic Engineering from Edo State University, Ekpoma, Nigeria in 1998. Furthermore, he obtained M.Eng. in Electronic and Telecommunication Engineering and M.Sc. in Computer Science from the University of Benin, Benin-City, Nigeria in 2008 and 2006, respectively. Engineer Egbune is currently pursuing a Ph.D. in Telecommunication Engineering with the Department of Electrical and Information Engineering of Landmark University, Omu-Aran, Nigeria, where he is currently working as a lecturer. His research interest includes spatial modulation techniques for wireless communication, MIMO and large MIMO systems, optical communications, machine learning and image processing.

Babatunde Segun Adejumobi received his B.Sc. and M.Sc. degree in Electronic and Computer Engineering from the Lagos State University, Lagos, Nigeria in 2007 and 2012, respectively. Furthermore, he obtained a Ph.D. in Electronic Engineering from the Department of Electrical, Electronic and Computer Engineering of the University of KwaZulu-Natal, Durban, South Africa. Dr. Adejumobi is a reviewer for several international journals on wireless communication. He is registered Engineer with the Council for the Regulation of Engineering in Nigeria (COREN). His current research include spatial modulation techniques for wireless communications, space-time block coded modulation and orthogonal frequency division multiplexing. However, he is interested in optical communications, internet of things, machine learning and Image processing.

Isaac O. Avazi Omeiza received the B.Eng and M.Eng degrees in Electrical Engineering from University of Ilorin, Nigeria, in 1990 and 2000 respectively. He further obtained a Ph.D. in Electrical Engineering from the same university in 2007. His major research interests include: Image Analysis, Pattern recognition, Computer Vision and Digital Systems. He is presently a member of faculty in the Department of Electrical and Information Engineering at Landmark University, Omu-Aran, Nigeria.

Francis Ibikunle is a Professor of Information and Communication Engineering since 2013. He obtained his first degree in Electrical Engineering from the Rivers State University of Science and Technology, Port-Harcourt, Nigeria in 1986**.** In 1993, he won a Federal Government Scholarship award to study Information and Telecommunications Engineering at Beijing University of Posts and Telecommunications, Beijing, China where he obtained his Ph.D. in 1997. He is currently working at Landmark University, Omu Aran, Nigeria as a Researcher in the Electrical and Information Engineering. Prior to being an academic, he had worked in the industry. His work experience and area of expertise include Mobile & Wireless Communications, IoTs, Artificial Intelligence Techniques, Energy and Energy Efficiency. He has several publications to his credit in categories of dissertations, chapters in books, journal articles, and conference proceedings. He is an associate editor and editorial board member of at least 12 referred international journals. He is a registered member of several professional and academic bodies like the Council for the Regulation of Engineering in Nigeria (COREN), Nigerian Society of Engineers (MNSE), Nigerian Institution of Power Engineers (NIPE).

Oluwole Ayodele Sunday holds Bachelor of Engineering (B. Eng., 2003) degree from the University of Ado – Ekiti *Now* Ekiti – State University, Master of Engineering (M. Eng., 2010) degree from Federal University of Technology, Akure, and Doctor of Philosophy (PhD, 2018) degree from the University of KwaZulu – Natal, South Africa. Professionally, Dr. Oluwole is a registered Engineer with the Council for the Regulation of Engineering in Nigeria (COREN). He is a Lecturer at the department of Electrical and Electronics Engineering, Federal University Oye-Ekiti, Ekiti State, Nigeria.

Thokozani Shongwe received the B. Eng degree in Electroinc engineering from the University of Swaziland, Swaziland, in 2004 and the M.Eng degree in Telecommunications Engineering from the University of the Witwatersrand, South Africa, in 2006 and the D. Eng degree from the University of Johannesburg, South Africa, in 2014. He is currently an Associate Professor at the University of Johannesburg, department of electrical and electronic engineering Technology. He is a recipient of the 2014 University of Johannesburg Global Excellence Stature (GES) award, which was awarded to him to carry out his postdoctoral research at the University of Johannesburg. In 2016, Prof T. Shongwe was a recipient of the TWAS-DFG Cooperation Visits Programme funding to do research in Germany. Other awards that he has received in the past are: the post-graduate merit award scholarship to pursue his master's degree at the University of the Witwatersrand in 2005, which is awarded on a merit basis; In the year 2012, Prof. Shongwe (and his co-authors) received an award of the best student paper at the IEEE ISPLC 2012 (power line communications conference) in Beijing, China. Prof T. Shongwe's research fields are in Digital Communications and Error Correcting Coding. His research interests are in power-line communications; cognitive radio; smart grid; visible light communications.